Int. J. Heat Mass Transfer. Vol. 14, pp. 697–707. Pergamon Press 1971. Printed in Great Britain

EDDY DIFFUSIVITY OF MASS MEASUREMENTS FOR AIR IN CIRCULAR DUCT

N. SHERIFF and D. J. O'KANE
Reactor Engineering Laboratories, U.K.A.E.A., Risley, Lancashire, England

(*Received* 4 *May* 1970 *and in revised form* 26 *August* 1970)

Abstract—Continuous injection of a tracer gas (nitrous oxide) on the centreline of a circular duct has been used to measure the eddy diffusivity of mass for turbulent air flow. Using axial concentration distributions the limitations of the 'point source' solution have been revealed, and a modified evaluation procedure has been used.

For the Reynolds number range tested, $1{\cdot}3 \times 10^4$–$1{\cdot}3 \times 10^5$, the eddy diffusivity of mass in the central region of the tube was found to be:

$$\frac{\varepsilon_{Ma}}{\nu} = 25{\cdot}27\, Re\,.\,10^{-4} - 3{\cdot}82.$$

Using eddy diffusivities of momentum from previous studies, the turbulent Schmidt number varied between 0·7 and 1·0.

NOMENCLATURE

a, height of rectangular duct [cm];
C, concentration of tracer gas;
D, molecular diffusivity [cm^2/s];
d, diameter of circular duct [cm];
f, friction factor, defined: pressure drop $\div\ \rho\,.\,(\bar{u})^2\,.\,(2x/d)$;
L, either a or d used in evaluating P [cm];
l_m, mixing length in turbulent flow [cm];
q_0, rate of tracer gas injection [cm^3/s];
r, direct distance from source to sampling position [cm];
t, time [s];
T, timescale required for one mean free path l_m/u' [s];
$\bar{u}$, mean channel velocity [cm/s];
u', turbulent velocity component in x-direction [cm/s];
x, axial distance from source in flow direction [cm];
x_i, axial position of virtual source [cm];
x_T, axial movement in time T [cm];
y, distance from duct wall [cm].

Dimensionless groups
Pr, Prandtl number, ν/α;
Re, Reynolds number, $\bar{u}\,.\,d/\nu$;
Sc, Schmidt number, ν/D;
Sc_T, turbulent Schmidt number, $\varepsilon_M/\varepsilon_{Ma}$;
P, defined as: $\bar{u}\,.\,L/\varepsilon_{Ma}$, where $L = a$ or d.

Greek symbols
α, thermal diffusivity [cm^2/s];
ε_H, eddy diffusivity of heat [cm^2/s];
ε_{Ma}, eddy diffusivity of mass [cm^2/s];
ε_M, eddy diffusivity of momentum [cm^2/s];
ε_p, eddy diffusivity of marked particles [cm^2/s];
ρ, fluid density [g/cm^3];
ν, fluid kinematic viscosity [cm^2/s];
τ_0, wall shear stress [dynes/cm^2];
τ_T, turbulent shear stress [dynes/cm^2].

1. INTRODUCTION

THE MEASUREMENT, in air, of the eddy diffusivity of mass has been the subject of several investigations in the past, e.g. [1–9]. In addition to the deviations from one investigation to another, there have been cases where the scatter of the experimental values has been large in an individual study. Several factors probably contribute to this situation.

In the first case, experimental techniques have varied. The majority of the studies have involved the eddy diffusivity in the central region of a duct. An injector placed on the centreline of the duct provides a tracer gas, and the evaluations are based on measured concentration profiles downstream of the injector. Within this basic scheme it is possible to have different arrangements; for example the size of the injector has been varied, c.f. [6] and [8] where in approximately the same duct size (~ 100 mm) injectors of 1·1 mm and 25 mm dia. were used respectively. Another variable is the measuring position relative to the injector; again cf. [1] and [6] where measurements were made at average distances of 10 and 50 pipe diameters from the injector respectively. It is also possible that the rate of injection of the tracer gas could affect the measurements. Emphasis on the upstream distance of undisturbed flow has always been made by experimentalists, and with most of the studies using at least 20–30 pipe diameters upstream of measuring positions it is unlikely that errors have been produced by this effect.

Secondly, different tracer gases have been used in the various experiments. Only recently [7] has attention been focused on the effect of the gas used, and since the Schmidt number is thus affected, variations in measured eddy diffusivities of mass are likely. Similar to the allied heat transfer situation, where the effects of Prandtl number are not fully understood, it is not possible to allow for Schmidt number precisely.

The purpose of the present study was to investigate the likely causes of the discrepancies in the measured values of the eddy diffusivity of mass in air. A circular duct, with nitrous oxide injected through a hypodermic tube on the centreline, was used. The Reynolds number range was $1{\cdot}3 \times 10^4$–$1{\cdot}3 \times 10^5$. Detailed measurements of axial concentration distributions have been made, together with radial distributions. The evaluation of the eddy diffusivity for the central region is discussed with respect to these measurements, and in particular the relevance of the 'point source' solution is assessed.

Use has been made of the measured values of the eddy diffusivity of momentum by Quarmby [6] to evaluate a turbulent Schmidt number, and comparison with the theoretical predictions of $\varepsilon_m/\varepsilon_H$ [10–12] has been made.

2. EXPERIMENTAL APPARATUS

The rig consists of a vertical 76·5 mm (i.d.) copper tube with an orifice plate to meter the air flow, and a similar downcomer which contains the test section. These two legs of the rig are linked by a 25 mm dia. tube, with the change of cross-section to the test section achieved by means of a diffuser section. To establish the turbulent field a total distance of about 30 pipe diameters separates the inlet to the downcomer and the first measuring positions on the test section. A flow diagram of the rig is shown in Fig. 1.

The test section consists of an injector tube of 2 mm o.d. centralised in the copper pipe by fine wires. The injector tube extends for 270 mm along the pipe centreline, and pure nitrous oxide or a nitrous oxide–air mixture was injected concurrently into the main channel flow. A sampling head, consisting of flattened hypodermic tubing, was used to measure the concentration profiles at various axial positions downstream of the injector.

Concentration profiles were measured using an I.R.D. infra-red gas analyser. Test section flow rates were measured using standard orifice plates designed to B.S.1042; injector flow rates were measured with rotameters. The main channel temperature was checked with a thermocouple.

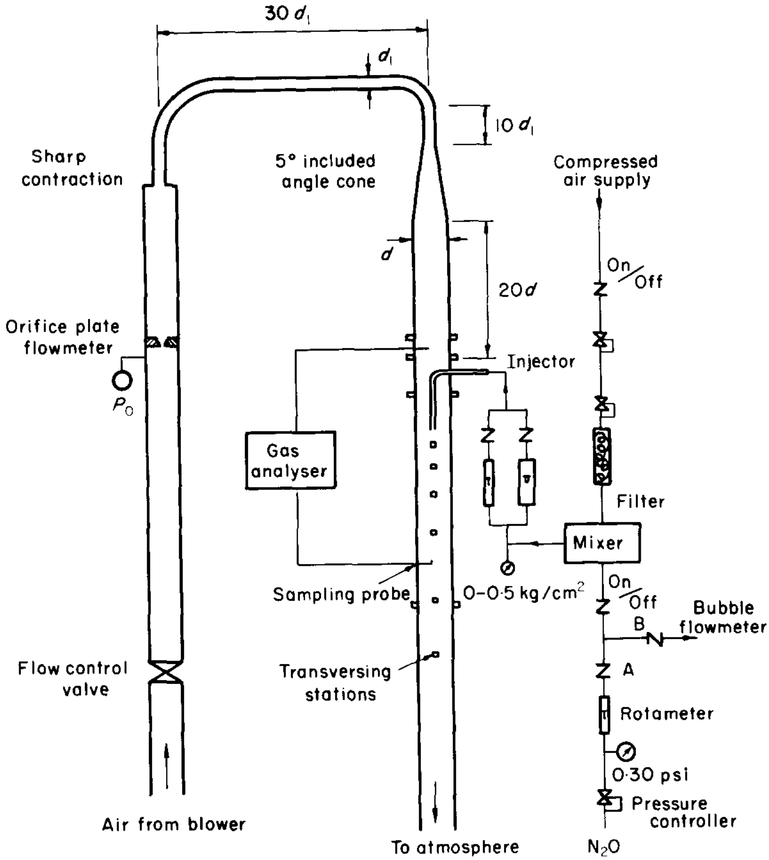

FIG. 1. Apparatus flow diagram.

2.1 *Details of experimental technique*

To ensure accuracy in the use of the gas analyser it was found necessary to vary the mixture ratio injected. In this way a reasonable fraction of the full-scale reading on the analyser was obtained, thus ensuring maximum accuracy. The rotameter measuring the nitrous oxide flow was calibrated with a bubble flowmeter at ambient temperature. A correction to allow for the rig temperature conditions was applied to the rotameter measurements. Any errors likely to be caused by background concentration effects were eliminated by purging the gas analyser with air from a position upstream of the injector.

In the experiments the main emphasis was placed on measurements of the axial concentration distribution on the tube centreline. To ensure that the maximum concentration was measured at each axial station, detailed traverses were done at 1 mm intervals in the region around the tube centreline.

Anticipating effects of the velocity of the injected tracer gas preliminary measurements were made in which this velocity was varied. For injector velocities in the range +30 per cent to −50 per cent of the mean channel velocity there was a negligible effect on the measured eddy diffusivity. Thus it was not necessary to set precise values of the injector flow during the experiments.

3. ANALYSIS OF EXPERIMENTAL DATA

The basis of the analysis was originally in the field of heat transfer, where Wilson [13] solved the temperature conditions for a continuous point heat source in an infinite fluid stream moving with uniform velocity. Towle and Sherwood [1] modified this analysis to the measurement of eddy diffusivity of mass in a duct and obtained:

$$C = \frac{q_0}{4\pi\, \varepsilon_{Ma} r} \exp - \left[\frac{\bar{u}}{2\varepsilon_{Ma}}(r - x)\right]. \quad (1)$$

This was re-written to give:

$$\ln(C.r) - \ln(\alpha) = -\beta(r - x) \quad (2)$$

where

$$\alpha = \frac{q_0}{4\pi\varepsilon_{Ma}} \quad \text{and} \quad \beta = \frac{\bar{u}}{2\varepsilon_{Ma}}.$$

Plotting ln $(C.r)$ against $(r - x)$ enables all of the measured data to be represented on the same graph, and two values of ε_{Ma} can thus be obtained. The intercept on the ln $(C.r)$ axis enables the "intercept" value of ε_{Ma} to be calculated and represents all of the centre-line concentration measurements. The slope of the line similarly leads to the "slope" value of ε_{Ma}, which represents measurements made at various radial positions from the tube centre-line. Because the conditions to which equation (1) applies are not strictly applicable in the present experiment it is felt that the analogy could only be approximately true. For example, a point source is not used, the velocity is not uniform in the central region and the eddy diffusivity is not necessarily constant across the channel.

In the present study it has been found necessary to modify the above analysis to include only the peak concentration data. From equation (1), the relationship between the concentration on the duct centreline and axial position from the source is given by:

$$\frac{1}{C} = \left[\frac{4\pi\,.\,\varepsilon_{Ma}}{q_0}\right] x. \quad (3)$$

The point source solution given by equation (3) would give a straight line through the origin on a plot of $(1/C)$ against x. As the results will show, and the simple analysis in Appendix 1 indicates, the straight line does not pass through the origin. Misleading results were initially found from the use of equations (1) and (2), and the results have been evaluated from the the slope of the $(1/C)$ vs. x plot at positions distant from $x = 0$. The magnitude of this has been shown in Appendix 1 to be equal to:

$$\frac{4\pi\varepsilon_{Ma}}{q_0}. \quad (4)$$

4. EXPERIMENTAL RESULTS

Two methods, as noted in the previous section, are available for the evaluation of ε_{Ma} from the experimental measurements. That used by Towle and Sherwood [1] involving a plot of ln $(C.r)$ against $(r - x)$ produces both an "intercept" and "slope" value for ε_{Ma}. In the present experiments a considerable variation of ε_{Ma} with axial distance from the injector was noted, see Fig. 2. Consequently the second method given in section 3 was adopted.

This involves the use of the centre-line concentration measurements only; the reciprocal of the concentration being plotted aginst x as shown in a typical set of results in Fig. 3. The fact that the asymptotic line at large values of x does not pass through the origin explains the inadequacy of the first method, since for equations (1) and (2) to be valid this would be necessary.

All of the results have been evaluated using this second method, where the asymptotic slope is given by expression (4). The effect of the mean channel velocity on the axial concentration distribution is shown in Fig. 4, and the evaluated values of (ε_{Ma}/ν) as a function of

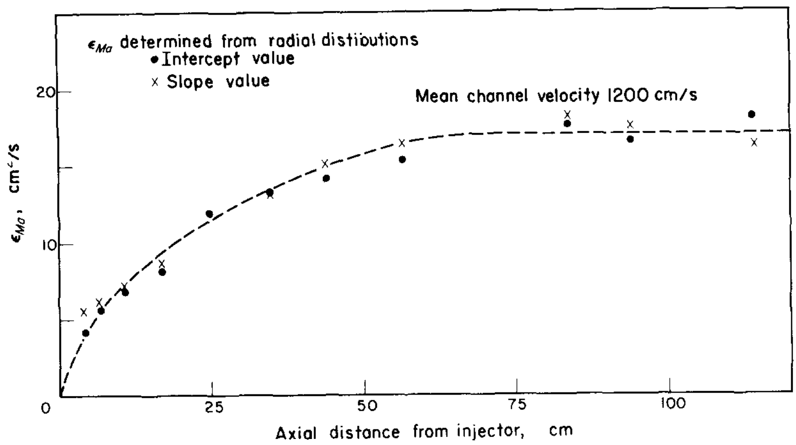

FIG. 2. Axial variation of ε_{Ma} with point source analysis.

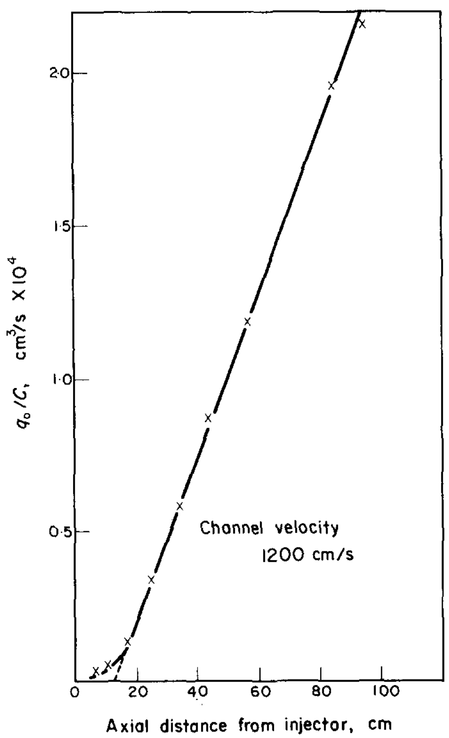

FIG. 3. Typical axial concentration distribution.

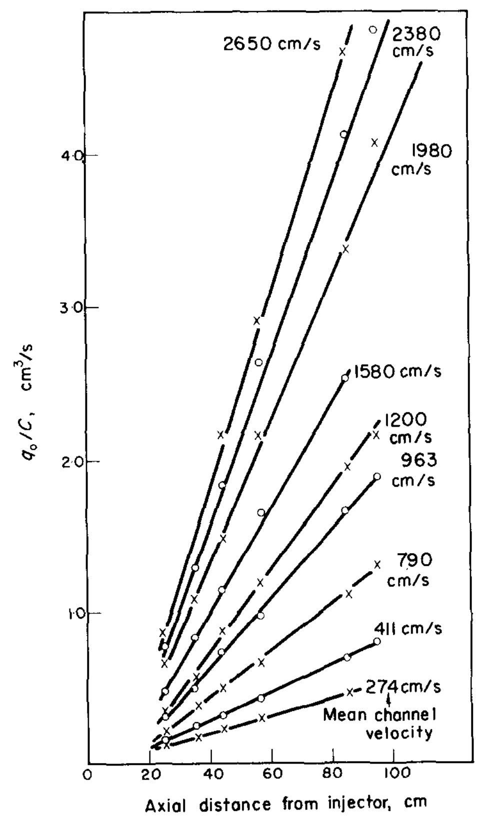

FIG. 4. Variation of axial concentration with channel velocity.

Reynolds number are given on Fig. 5. Assuming a linear relationship, the 'best-line' fit for these results is given by:

$$\frac{\varepsilon_{Ma}}{\nu} = 25{\cdot}27\,(Re\,.\,10^{-4}) - 3{\cdot}82.$$

Calculated friction factors from pressure drop measurements in the tube agreed with smooth tube values.

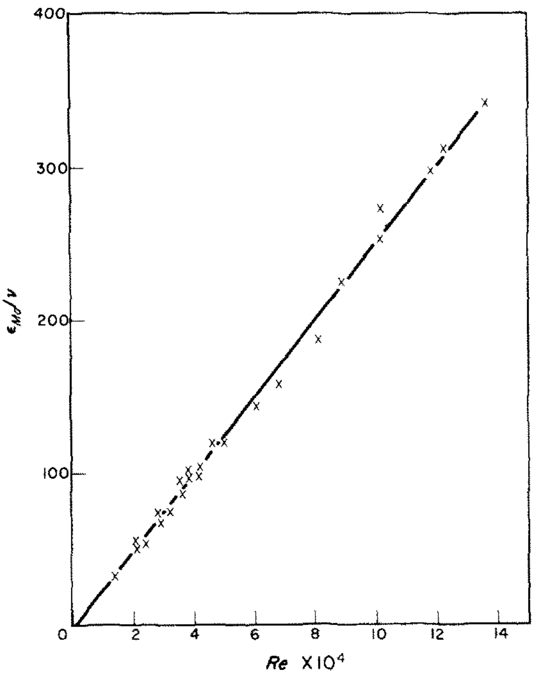

FIG. 5. Variation of ε_{Ma}/ν with Reynolds number.

5. DISCUSSION OF RESULTS

5.1 *Comparison with previous work*

A comparison of the results with those of other workers is shown in Fig. 6, where the dimensionless parameter P is given as a function of Reynolds number. The parameter P, sometimes referred to as the turbulent Péclét number, is used because it enables comparisons to be made with parallel plate configurations. Since (ε_{Ma}/ν) is virtually proportional to Reynolds number from the present results, P does not vary with Reynolds number. Since Quarmby [6] also used nitrous oxide as the tracer gas, a comparison with these results is particularly relevant. An average value of P from the present work is 410, whilst Quarmby's results give an average value of 530. The deviation between the two sets of results is thus approximately 20 per cent. Since the experimental accuracy of the measurement of ε_{Ma} is usually about $\pm$ 10 per cent, it is possible that the discrepancy between the results is not serious.

Towle and Sherwood [1] have reported values of the mass diffusivity obtained by injecting hydrogen and CO_2 from a point at the axis of various circular ducts. Radial concentration profiles were measured using a fixed array of sampling tubes and the diffusivity values were calculated using the logarithmic form of the Wilson equation (2). Their results compared with those now reported gave lower values of ε_{Ma}, see Fig. 6, where *higher* P values represent *lower* ε_{Ma} values. They found that their intercept and slope values increased asymptotically with distance from the injector point and it would seem likely that the true asymptote was never reached. From the present work, it would appear that even at $x/d \sim 12$ the error incurred by the assumption of the point source equation is 10 per cent. Since the point source equation was used in [1] with a configuration such that $x/d \sim 10$, it is possible that the evaluation of ε_{Ma} would give low values.

A further point to note in the results of Towle and Sherwood [1] was the lack of sensitivity of the values of ε_{Ma} on the tracer gas used. Since the Schmidt number is vastly different for hydrogen and carbon dioxide, some effect similar to that noted by other workers [7] would have been expected.

The results obtained in a rectangular duct of high aspect ratio have been reported by Clanachan [9]. Defining the parameter P in terms of the height of the duct and not the hydraulic diameter, see Appendix 2, provides results for direct comparison with circular duct data.

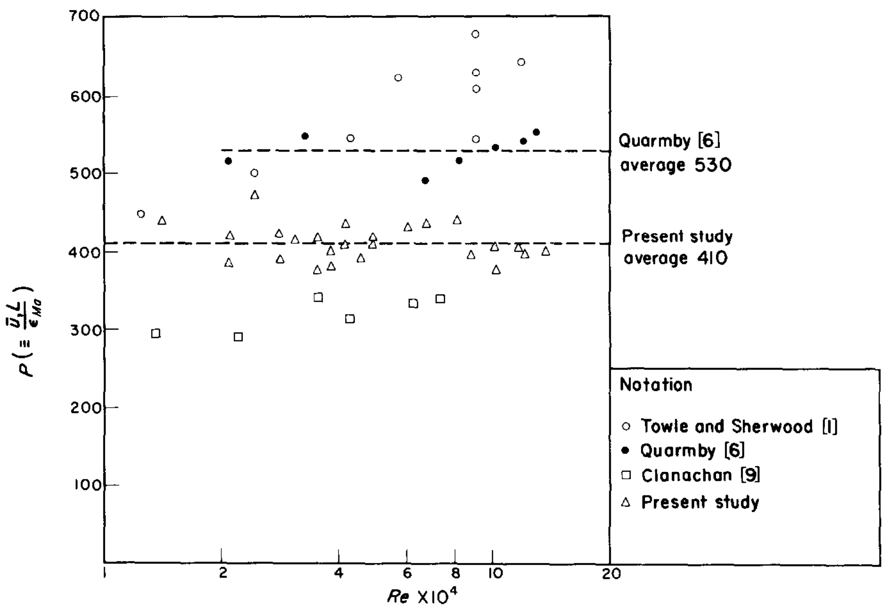

FIG. 6. Parameter P as function of Reynolds number.

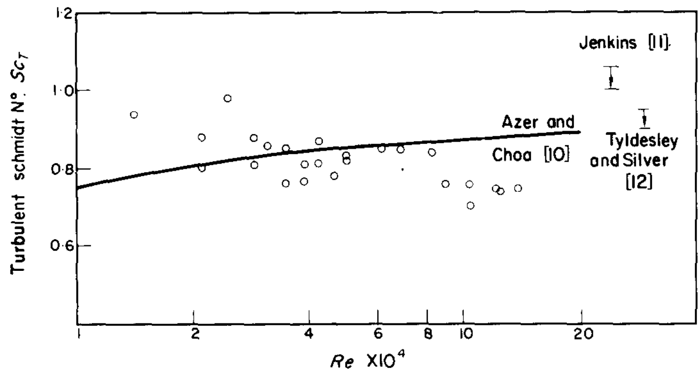

FIG. 7. Turbulent Schmidt number as function of Reynolds number.

The results of [9] are shown to give lower values than the present data, see Fig. 6.

5.2 *Turbulent Schmidt number*

Measurements of the eddy diffusivity of momentum were not made in the present study, and the results of Quarmby [6] have been adapted to evaluate the turbulent Schmidt number, Sc_T. Quarmby measured point values of ε_M and mean values in the central region have been derived from his distributions. These values show reasonable agreement with those of Hinze [14]. The turbulent Schmidt number evaluated from the present work is shown in Fig. 7 as a function of Reynolds number; the values range from 0·7 to 1·0. Theoretical predictions of $\varepsilon_M/\varepsilon_H$ have been made by Jenkins [10], Azer and Choa [11] and Tyldesley and Silver [12] of the effect of Prandtl number. By analogy these can be interpreted as turbulent

Schmidt numbers in terms of the molecular Schmidt number. The value of Sc for nitrous oxide in air is 0·77, and the theoretical predictions are shown in Fig. 7. The best agreement appears to be with the Azer and Choa predictions, although the differences from the other theories are probably within the accuracy claimed of these analyses.

5.3 *Differences from 'point source' solution*

The deviation of the measurements from the 'point-source' predictions is an interesting feature; this is clearly seen in the axial concentration distributions. It is thought that this discrepancy is significant and may be explained by reference to the simpler turbulence theories.

Using the phenomenological theories of turbulence, which represent turbulence in terms of mixing lengths and mean transverse velocity components, an explanation of certain features of the results is possible. Details are given in Appendix 1 where the main assumption made is that there is an initial time delay in the diffusion process before the movement of the fluid particles become fully effective. This time delay is assumed to be of the same order as the time taken for fluid particles to travel a distance equal to the mixing length (l_m), with a velocity equal to the turbulent component (u'). Since in the present technique time is represented by the axial distance downstream of the injector together with the mean pipe velocity, it is shown that the equivalent distance downstream before diffusion is fully effective can be represented as an intercept on the x axis:

$$x_i = x_T = \frac{\bar{u}\varepsilon_M}{(u')^2}.$$

Using Hinze's [14] expression for ε_M:

$$\frac{x_i}{d} \simeq \frac{0{\cdot}055}{\sqrt{(f/2)}} \tag{5}$$

which at $Re = 6 \times 10^4$ gives $x_i/d = 1{\cdot}1$.

In the pipe diameter used in the tests the distance downstream of the injector (x_i) is 8 cm. This value is in good agreement with the intercept obtained from the axial distribution in Fig. 3, and thus helps to confirm that the effect is real and not a function of the experiment. It has been noted that Hinze [14] reports similar results from measurements with a line source. In a much more exact analysis he obtained similar results for the intercept effect.

6. CONCLUSIONS

1. The evaluation of the eddy diffusivity of mass from concentration measurements downstream of a continuous injection of tracer gas is not straightforward, since axial concentration profiles have shown that the simple 'point source' solution does not apply.

2. The measured values of ε_{Ma} for the tube central region can be represented by either of the following relationships:

$$\text{(a)}\ \frac{\varepsilon_{Ma}}{\nu} = 25{\cdot}27\, Re\,.\,10^{-4} - 3{\cdot}82$$

or

$$\text{(b)}\ \frac{\bar{u}\,.\,d}{\varepsilon_{Ma}} = 410.$$

3. The turbulent Schmidt number when nitrous oxide is used as tracer gas in the air ($Sc = 0{\cdot}77$) was found to vary between 0·7 and 1·0.

ACKNOWLEDGEMENTS

Mr. D. A. Greene was involved in the earlier experimental work which preceded this final investigation.

This paper is published by permission of the Managing Director of the Reactor Group of the United Kingdom Energy Authority.

REFERENCES

1. W. L. TOWLE and T. K. SHERWOOD, Mass transfer in the central portion of a turbulent air stream, *Ind. Engng Chem.* **31**, 457 (1939).
2. T. K. SHERWOOD and B. B. WOERTS, The role of eddy diffusion in mass transfer between phases, *Trans. A.I.Ch.E.* **35**, 517 (1939).
3. D. L. FLINT, H. KADA and T. J. HARATTY, Point source turbulent diffusion in a pipe, *A.I.Ch.E. Jl* **6**, 325–331 (1960).
4. H. A. BECKER, R. E. ROSENWEIG and J. R. GWOZDZ, Turbulent dispersion in a pipe flow, *A.I.Ch.E. Jl* **12**, 964 (1966).

5. C. BETTS and A. P. HATTON, To be published in *Proc. Inst. Mech. Engrs*.
6. A. QUARMBY and R. K. ANAND, Axisymmetric turbulent mass transfer in a circular tube, *J. Fluid Mech.* **38**, 433 (1969).
7. I. B. GOLDMAN and J. M. MARCHELLO, Turbulent Schmidt numbers, *Int. J. Heat Mass Transfer* **12**, 797–802 (1969).
8. W. G. SCHLINGER and B. H. SAGE, Material transfer in turbulent gas streams, *Ind. Engng Chem.* **45**, 657 (1953).
9. D. CLANACHAN, The enhancement of turbulent mixing in air flows in a rectangular duct, M.Sc. Thesis, U.M.I.S.T. (1968).
10. R. JENKINS, Variation of eddy conductivity with Prandtl modulus and its use in prediction of turbulent heat transfer coefficient. Heat Transfer and Fluid Mechanics Preprints, Stanford Univ. Press., Palo Alto, Calif. (1951).
11. N. Z. AZER and B. T. CHOA, A mechanism of turbulent heat transfer in liquid metals, *Int. J. Heat Mass Transfer* **1**, 121 (1960).
12. J. R. TYLDESLEY and R. S. SILVER, The prediction of the transport properties of a turbulent fluid, *Int. J. Heat Mass Transfer* **11**, 1325–40 (1968).
13. H. A. WILSON, On convection of heat, *Proc. Camb. Phil. Soc.* **12**, 406 (1904).
14. J. O. HINZE, *Turbulence*. McGraw-Hill, New York (1959).
15. J. LAUFER, The structure of turbulence in fully developed pipe flow, NACA Tech. Report No. 1174 (1954).

APPENDIX 1

Discrepancy from Point Source Predictions

As the axial concentration distributions showed, the point source solution did not apply at the axial positions immediately downstream of the injection position. In this appendix a simple explanation based on mixing-length theories is indicated, and results from a more exact statistical analysis will be quoted in support.

Turbulence represents a random motion of the fluid. Consider a random motion in the y-direction of marked fluid particles (M), such that a particle moves a fixed distance (mean free path) before changing direction. It can be shown that after several mean free paths have been covered the position of the marked particles can be expressed by:

$$\frac{dM}{dt} = D \cdot \frac{d^2M}{dy^2} \qquad (A.1)$$

where D = diffusion coefficient.

For turbulent flow the diffusion coefficient is referred to as the eddy diffusivity, and from the phenomenological theories of turbulence the definitions of the eddy diffusivity of momentum and mixing length are noted:

$$\varepsilon_M = \frac{\tau_t}{(du/dy)} - \nu$$

$$l_M = \frac{u'}{(du/dy)}.$$

Now $\tau_t = \rho - \varepsilon_m(du/dy) = \rho \,.\, \overline{u'v'}$, and assuming that $u' \sim v'$ the following expression for ε_m is obtained:

$$\varepsilon_M = l_M^2(du/dy) = l_M \,.\, u'. \qquad (A.2)$$

This has the same form as the diffusion coefficient obtained from the kinetic theory of gases, with l_M replacing the distance between collisions and u' the mean molecular velocity.

As noted earlier, the representation of the motion by a coefficient of diffusion depends upon the time of diffusion being sufficiently long for the particles to have traversed several mixing lengths. If $T(\sim l_M/u')$ represents the time of a particle to traverse one mixing length, then the requirements for the above conditions are that the timescale of the motion is greater than T.

Considering the timescale of the particle motion to be less than T, whilst assuming that equation (A.1) represents the particle motion. In Fig. 8 the distribution of M as a function of y is shown, where M_1 and M_2 represent values one

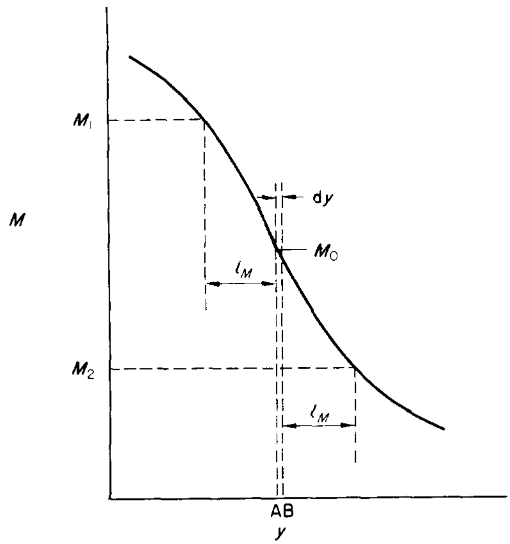

FIG. 8. Distribution of marked particles.

mean free path from the small cell dy. If n is the number of particles entering and leaving dy in the planes A and B, then for this cell for long timescales ($t > T$) we have:

$$\frac{dM}{dt} = n[(M_1 + M_2) - 2M_0] = \varepsilon_p \cdot \frac{d^2M}{dy^2}. \qquad (A.3)$$

With a short timescale, ($t < T$), however, the particles entering dy will be less than $n(M_1 + M_2)$. Thus if a coefficient of diffusion is retained as defined in (A.3) its value will be less than that given for longer timescales. Alternatively this has sometimes been expressed as a diffusion coefficient which varies with time when $t < T$.

As a consequence any attempt to measure the eddy diffusivity in the period immediately after diffusion has started will give false results. In the present experiment this represents axial positions near to the point of injection, and transforming T into an axial distance one obtains:

$$x_T = \frac{l_M}{u'}\bar{u} = \frac{\bar{u}\,.\,\varepsilon_{Ma}}{(u')^2}.$$

Using the value of u' obtained by Laufer [15] and assuming that $\varepsilon_{Ma} = \varepsilon_M$, the later given by Hinze's expression $\varepsilon_M = 0{\cdot}035\,\bar{u}d\sqrt{f/2}$, x_T becomes:

$$x_T = \frac{\bar{u}\,0{\cdot}035\,\bar{u}\sqrt{(f/2)}\,.\,d}{[0{\cdot}8\,\bar{u}\sqrt{f/2}]^2} = \frac{0{\cdot}055\,(d)}{\sqrt{f/2}}. \tag{A.4}$$

Statistically on the concentration distribution centre line a time equivalent to two mean free paths is necessary before the variation with time is random. Thus a $1/C$ vs. x-plot would not be linear until $x = 2x_T$, and the intercept with the x-axis must then lie between $x = 0$ and $x = 2x_T$.

Assuming the intercept to equal x_T, at $Re = 6 \times 10^4$ this gives an intercept of 8 cm; compared to the measured values ~ 10 cm. The agreement is good, and it is considered that the measured intercept on the x-axis is real and caused by the turbulence structure in the pipe. In effect the intercept position x_T represents a virtual origin for the axial concentration distribution at large distances.

APPENDIX 2

Comparison of Circular and Rectangular Duct Diffusivities

The appendix outlines the reasoning behind the increased eddy diffusivity in a circular duct compared with a rectangular channel at the same Reynolds number.

For a circular duct the eddy diffusivity of momentum can be calculated from the universal velocity profile to be:

$$\frac{\varepsilon_M}{\nu} + 1 = 0{\cdot}40\left(1 - \frac{2y}{d}\right)\frac{y}{d}\sqrt{(f/2)}\,\mathrm{Re}.$$

For a rectangular duct of height a, the universal velocity profile predicts the following expression for ε_M:

$$\frac{\varepsilon_M}{\nu} + 1 = 0{\cdot}20\left(1 - \frac{2y}{a}\right)\frac{y}{a}\sqrt{(f/2)}\,Re.$$

Thus at the same Reynolds number and at geometrically similar positions, i.e. the same value of y/d and y/a. The value of ε_M in a circular duct is twice that for the rectangular duct.

Replacing ε_M by ε_{Ma} it is thus possible to write:

$$\left[\frac{Re}{\varepsilon_{Ma/\nu}}\right]_{\text{Circular}} = \left[\frac{Re}{2\,.\,\varepsilon_{Ma/\nu}}\right]_{\text{Rectangular}}$$

i.e.

$$\left[\frac{\bar{u}\,.\,d}{\varepsilon_{Ma}}\right]_{\text{Circular}} = \left[\frac{\bar{u}\,.\,a}{\varepsilon_{Ma}}\right]_{\text{Rectangular}}$$

Comparison of eddy diffusivity data for the two ducts is possible in terms of the dimensionless parameter $\{\bar{u}\,.\,L/\varepsilon_{Ma}\}$, where L is either the diameter or the channel height for circular or rectangular ducts respectively.

MESURE DE LA DIFFUSIVITÉ DE MASSE PAR TURBULENCE CONCERNANT L'AIR DANS UN CONDUIT CIRCULAIRE

Résumé— On a utilisé, afin de mesurer la diffusivité de masse par turbulence pour un écoulement d'air turbulent, l'injection continue d'un gaz traceur (oxyde nitreux) sur l'axe d'un conduit circulaire. A partir de distributions axiales de concentration, les limitations de la solution "source ponctuelle" ont été révélées et un procédé d'évaluation modifiée a été utilisé.

Pour le domaine du nombre de Reynolds compris entre 1,3 . 10^4 et 1,3 . 10^5, la diffusivité de masse par turbulence dans la région centrale du tube est de:

$$\frac{\varepsilon_{Ma}}{\nu} = 25{,}27\,Re\,.\,10^{-4} - 3{,}82.$$

Utilisant les diffusivités par turbulence de quantité de mouvement contenues dans des études antérieures, le nombre de Schmidt turbulent varie entre 0,7 et 1.

MESSUNGEN DES TURBULENTEN STOFFAUSTAUSCHES FÜR LUFT IN ROHREN MIT KREISQUERSCHNITT

Zusammenfassung—Zur Messung des turbulenten Stoffaustauschkoeffizienten für eine turbulente Luftströmung wurde in die Mittelachse eines Rohres mit Kreisquerschnitt kontinuierlich ein Indikatorgas (Stickoxydul) eingeblasen. Mit Hilfe der axialen Konzentrationsverteilungen wurden die Grenzen der Lösung für die "punktförmige Quelle" aufgezeigt, und es wurde eine modifizierte Auswertungsmethode benutzt. Für den untersuchten Bereich der Reynoldszahl, von 1,3 . 10^4 bis 1,3 . 10^5, lässt sich der turbulente Stoffaustauschkoeffizient im Bereich der Rohrachse durch die Formel beschreiben:

$$\frac{\varepsilon_{Ma}}{\nu} = 25.27\,Re\cdot 10^{-4} - 3{,}82.$$

Bei Verwendung des turbulenten Impulsaustauschkoeffizienten aus früheren Untersuchungen bewegt sich die turbulente Schmidtzahl zwischen 0,7 und 1,0.

ИЗМЕРЕНИЯ КОЭФФИЦИЕНТА ВИХРЕВОЙ ДИФФУЗИИ МАССЫ ДЛЯ ВОЗДУХА В КРУГЛОМ КАНАЛЕ

Аннотация—Измерения коэффициента вихревой диффузии в турбулентном потоке воздуха проводились с помощью постоянного вдува трассирующего газа (двуокиси азота) по оси круглого канала. На основании распределения концентрации по оси установлены ограничения решения для «точечного источника», и тогда используется модифицированный метод расчета.

Для исследованного диапазона чисел Рейнольдса, $1,3 \times 10^4$–$1,3 \times 10^5$, найдено, что коэффициент вихревой диффузии для центральной области трубы равен

$$\frac{\varepsilon_{Ma}}{\nu} = 25,27\, Re \,.\, 10^{-4} - 3,82.$$

При использовании коэффициентов турблентной кинематической вязкости, взятых из проведенных ранее исследований, получен турбулентный критерий Шмидта от 0,7 до 1,0.